

Determination of the Lift and Drag of 2D Planing Flat Plate Riding on the Free Surface

Amin Rezaei, Hassan Ghassemi, Esmail Noshadi,

Department of Maritime Engineering, Amirkabir University Of Technology, Tehran, Iran

* Corresponding author email: gasemi@aut.ac.ir

Paper History

Received: 12-December-2015

Received in revised form: 28-December-2015

Accepted: 30-December-2015

ABSTRACT

The behavior of planing hull is very similar to planing flat plate. So to treat the planing hull performance at moderate Froude number, 2D planing flat plate was analyzed in different Froude number between 0.5 and 1. Finite volume, using ANSYS-CFX v14 software with RNG turbulence model was used to simulate planing plate. The numerical results of the pressure distribution, free surface profile, lift and drag at different AOAs are presented and discussed. Present calculations are compared with Kramer et al [7] results and show almost good agreement.

KEY WORDS: 2D planing flat plate, RNG turbulence model, Lift, Drag, Pressure distribution.

NOMENCLATURE

C_p	Pressure coefficient
D_t	Total drag
D_p	Pressure drag
D_w	Wave drag
D_s	Spray drag
D_f	Frictional drag
f	External force
g	Gravitational acceleration
Li	Initial immersed length
L_w	Wetted length ϵ_c Critical Strain
L_t	Total lift
L_s	Spray lift

L_p	Pressure lift
L_f	Frictional lift
u	Flow speed
U	Velocity vector
V	Pressure vector
λ	Wave length
μ	dynamic viscosity
μ_a	Air dynamic viscosity
μ_w	water dynamic viscosity
ν_a	Air kinematic viscosity
ν_w	Water kinematic viscosity
ρ	Density
ρ_a	Air density
ρ_w	Water density
τ	AOA (AOA)
τ_w	Wall shear stress

1.0 INTRODUCTION

Computational commercial software's play an important role in industry and economic system because investigators can reduce huge costs by using them. It is true that in marine industry experimental researches are particularly important but researchers can break costs and make more exact sample by simulation and refuse using wrong model tests. Hydrodynamic parameters and pressure distribution should be known to design a perfect planing hull. But planing hull treat like flat plate so forth investigators prefer to use planing flat plate instead of complex models to do their computational studies. 2-D planing flat plate surfaces are used for example as seaplanes, planing crafts, surface effect ship (SES) seals, thin foil without camber and water impact loads [1,2]. But in a number of these cases as SES seals, planing surface may operate at lower speeds where nonlinear effects are important and must be considered.

There are some experimental, analytical and numerical research in which the planing hull is considered as planing flat plate. Brown worked on the planing lift characteristics of rectangular flat plate and presented equations which calculate lift for all

deadrise angles [3]. Payne investigated very much on the planing flat plate and planing crafts, impact forces on those bodies, pressure distribution, etc. during 50 years from 1950-2000 [4, 5]. The influencing factors of drag reduction by air injecting to a flat-plate carried out by Ou and Dong [6].

A flow past a two dimensional flat plate at low Froude number was studied by Kramer et al (2013) [7]. The effects of viscosity and free-surface nonlinearity were concluded that nonlinear and viscous effects are important when the AOA is greater than approximately 10° and the low Froude number (means $Fr < 0.8$). Durante et al presented a numerical model for the 2D planing surfaces using linearized potential-flow theory at finite Froude number in which the surface is replaced by a representation of the pressure distribution along the plate using triangular pressure finite elements [8]. A simple numerical approach was employed to obtained data on hydrodynamic coefficients and flow pattern for various ranges of input parameters. These data are partly verified through the analysis of two limiting cases of the considered problem: first, the infinite depth, Froude number being finite and second, finite depth with very high Froude numbers [9]. The following sections are organized as follows. Section 2 is described the problem definition. Section 3 is given the modeling and boundary conditions and also computational domain. The governing equations are described in section 4. Section 5 presents the numerical results and discussions and finally conclusions are given in Section 6.

2.0 PROBLEM DESCRIPTION

In this study, two phase flow of air and water around a flat plat considering free surface was investigated. Schematic geometry of the planing flat plate is illustrated in Fig. 1. The planing plate length and thickness are 1m and 0.04m, respectively. Initial immersed length is $L_i=0.5m$. So the overall wetted length will be roughly $L_B=2L_i=1m$ based on reference [7]. A fixed reference coordinate system defined 2cm upper than leading edge. The plate has an AOA (τ). It is assumed that the flat plate has a constant speed of U on the free surface and the fluid is incompressible with a density and kinematic viscosity of ρ_w and ν_w , respectively. The flow speed U and AOA varied, whereas the other parameters were constant and pressure distribution, wave breaking and viscose resistance calculated based on Froude number at wet length of L_B . Different angles and speeds are presented in Table 1.

Table 1. The different angles and speeds used in this paper.

	Froude number	0.5	0.7	1.1
AOA (deg)	Speed(m/s)			
7.5	-	1.6	2.2	3.45
10	-	-	-	3.45
12	-	-	-	3.45
15	-	-	-	3.45

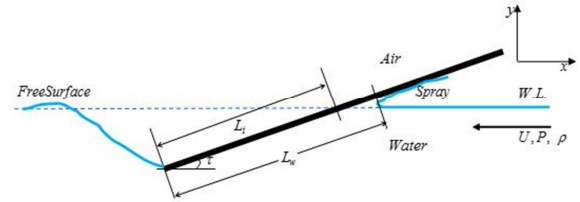


Figure.1: Problem definition.

3.0 MODELING AND BOUNDARY CONDITIONS

With attention to flat plat, computational domain should be $4L$ at upstream and $12L$ at downstream, where the L is plate length. The upper side (air) is $4L$ and lower side (water) is $4L$, as shown in Fig. 2. This domain was meshed by 145000 quad elements as shown in Fig. 3.

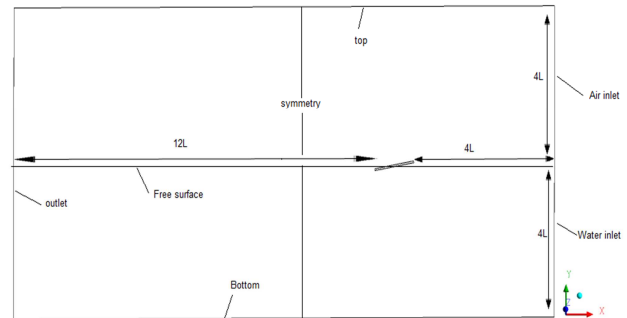


Figure.2: Domain dimensions and boundary conditions.

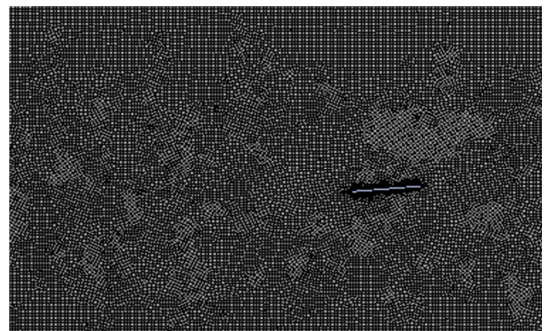


Figure.3: Computational mesh domain.

The size and type of elements play an important role in achieving correct results. To ensure that the results are not dependent to number of elements, the problem was solved for different numbers of element at AOA of 10° . As shown in Fig. 4, the lift and drag coefficients will be constant after 125000 elements and also pressure will converge based on Fig. 5 with this number of element. These two figure show that results are mesh independent.

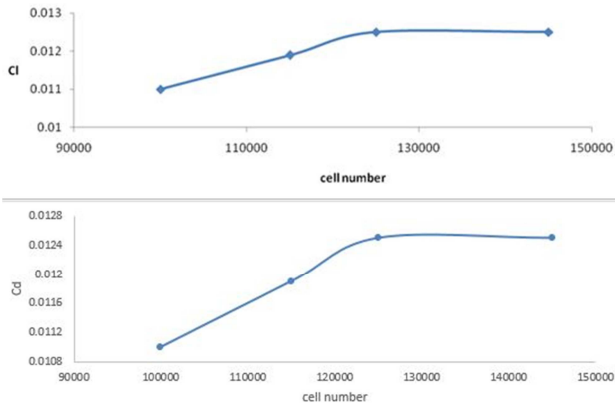


Figure.4: Effect of cell number on lift coefficient (AOA=10° and Fr= 1.1)

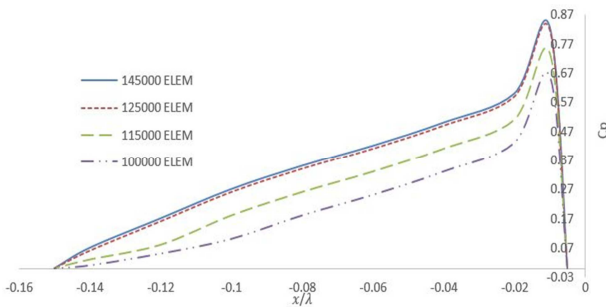


Figure.5: Convergence of pressure distribution on plate for various number of element, (AOA=10 deg, Fr=1.1)

4.0 GOVERNING EQUATION

To determine fluid treatment (velocity, pressure and free surface profile) all governing equations are given as follows:

- i. Continuity equation:

$$\nabla \cdot V = 0 \quad (1)$$

- ii. Navier-Stokes equations:

$$\rho \left(\frac{\partial V}{\partial t} + V \cdot \nabla V \right) = -\nabla P + \mu \nabla^2 V + f \quad (2)$$

Where "V" and "P" are velocity vector and pressure, respectively. In addition, the factor "f" denotes external forces.

- iii. Wall shear stress equation:

$$\tau = \mu \frac{\partial U}{\partial x} \quad (3)$$

where x refer to longitudinal direction. In order to obtain the volume fraction field in time, the following transport equation is

solved

$$\frac{\partial \alpha}{\partial t} + \nabla \cdot (u\alpha) = 0 \quad (4)$$

ANSYS-CFX software uses the volume fraction method to simulate the free surface. Volume fraction of a cell is its fraction of water. In this method water and air are consider as one specific fluid in which fluid density and viscosity change with parameter "a" in Eqs. (5) and (6). When a is 1 the whole cell is water and when it is 0 the whole cell is air.

$$\rho(X, t) = \alpha(X, t) \cdot \rho_w + (1 - \alpha(X, t)) \rho_a \quad (5)$$

$$\mu(X, t) = \alpha(X, t) \cdot \mu_w + (1 - \alpha(X, t)) \mu_a \quad (6)$$

The subscripts a and w denote air and water, respectively. In addition, x, t and μ are the spatial location vector, time variable and dynamic viscosity, respectively.

5. NUMERICAL RESULTS AND DISCUSSION

In order to validation the results, pressure coefficient is compared with Kramer et al results that reported in [7] at constant AOA $\tau = 7.5^\circ$ for various Froude numbers. Fig. 6 shows quite good agreement between simulation and Kramer's results, in which C_p and λ are:

$$C_p = \frac{P}{0.5 \rho_w u^2 L_w} \quad (7)$$

$$\lambda = \frac{2\pi u^2}{g} \quad (8)$$

where u is flow velocity in x-direction.

Hereafter, pressure distribution, free surface profile, list and drag are presented. Fig. 7 shows the pressure distribution at Fr=1.1 and AOA=10, 12 and 15 degrees. Waves generated of the free surface are shown in Figs. 8 and 9 at various AOA and Froude numbers. The height of wave and the length of wave, λ, increase by accretion in Froude number and AOA because of the relationship between flow speed and length of wave according to the equation (8). This cause in accretion of wave drag because wave energy is proportional to square of height according to equation (9) in which h is wave height.

$$E = \frac{1}{8} \rho * g * \lambda * h^2 \quad (9)$$

Also, it should be mentioned that when the AOA is increased more height of the wave generates at downstream of the flat plate. Because the flow separates from the trailing edge of the plate and causes more trough behind of the plate.

Fig. 10 illustrates contours of water velocity around plate. It is shown that velocity on the plate (near the wall) is zero because of no-slip boundary condition. Besides that, due to Fig 11 pressure is maximum in this region because of the decelerating of the velocity at leading edge of the flat plate. Lift and drag coefficients increase with Froude number and AOA. The major portion of lift and drag caused by pressure and viscose portion is neglect in comparison with pressure. This is a result of this fact that rate of

change of velocity ($\frac{\partial U}{\partial y}$) is negligible, as shown in Fig. 10.

Results of the lift and drag at various Froude number and various AOA are given in the Tables 3 and 4. The pressure drag and viscous drag components are also presented. Table 3 is given at various Froude numbers but the AOA is constant 7.5 deg. While Table 4 is shown the results at Fr=1.1 but AOA is 10, 12 and 15 degrees. The same data are presented in Figs. 12 and 13. Data of the Table 3 is demonstrated in Fig. 12 and Table 4 is related to Fig. 13.

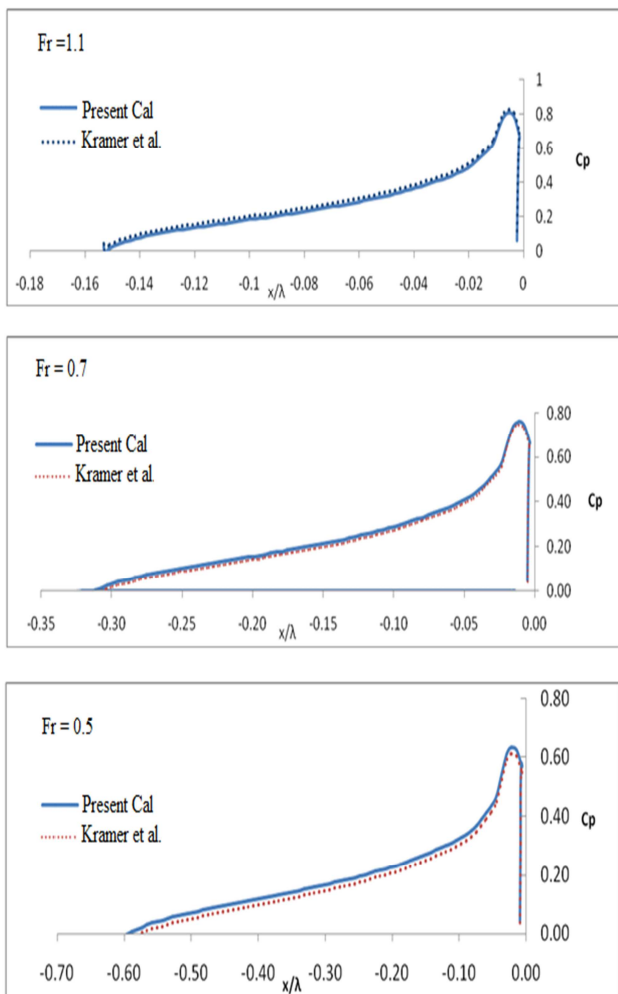


Figure.6: Comparison of pressure distribution coefficient between present calculation and Kramer et al. [7], AOA = 7.5°.

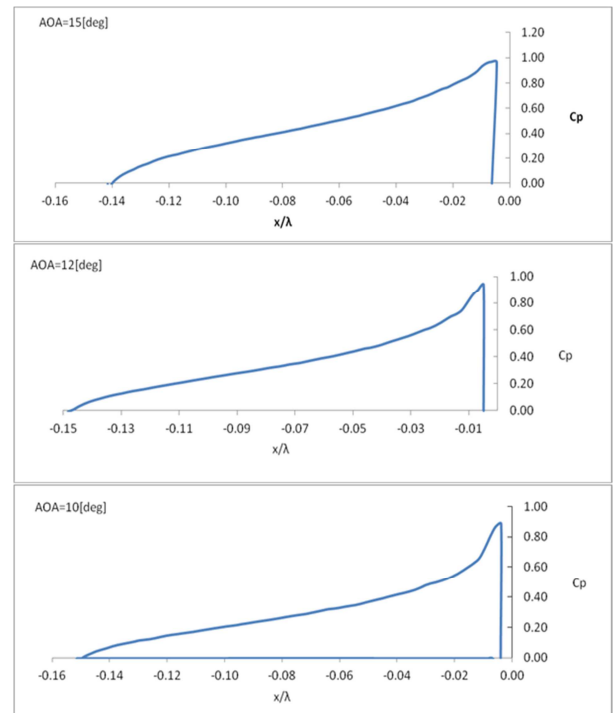


Figure.7: Pressure distribution coefficient as a function of plate length to wave length ratio for different AOA.

Table 3 Components of lift and drag in different Froude number (AOA = 7.5°)

Fr	Lift (N)	Pressure lift (N)	Drag (N)	Pressure drag (N)	Viscose drag (N)
0.5	21	21.16	9.8	9.76	0.05
0.7	28	28.07	12.1	11.39	0.04
1.1	35	36.01	15	14.97	0.03

Table.4: Components of lift and drag coefficient in different AOA (Fr=1.1.)

AOA [deg.]	Lift (N)	Pressure lift (N)	Drag (N)	Pressure Drag (N)	Viscose Drag (N)
10	63.98	64.04	16.66	16.32	0.34
12	72.02	72.07	20.24	20.04	0.2
15	97.67	97.72	30.2	29.9	0.3

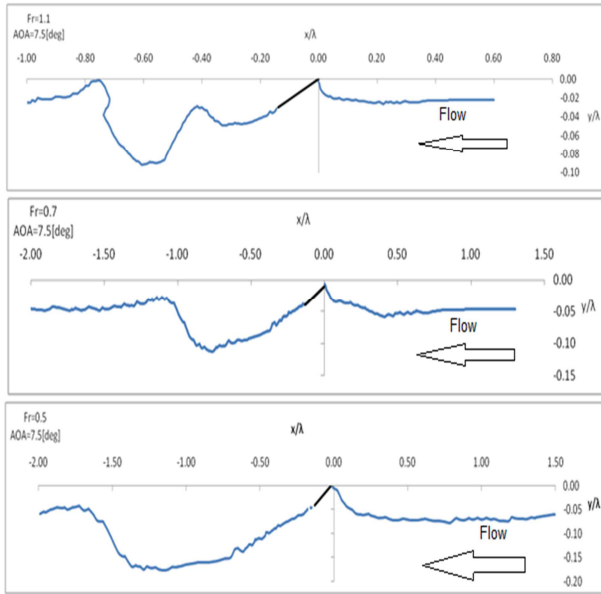


Figure.8: Plots of free-surface profile at different Fr, (AOA=7.5 deg)

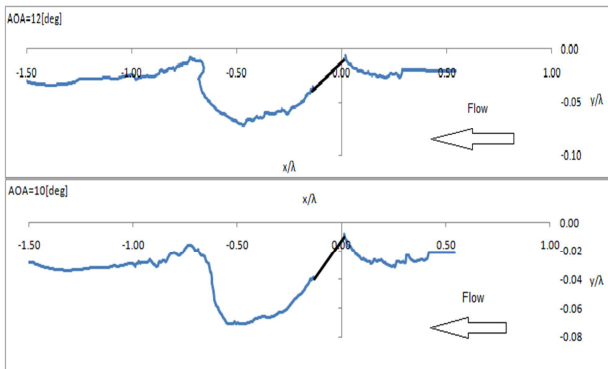


Figure.9: Plots of free-surface profile at different AOA (Fr=1.1)

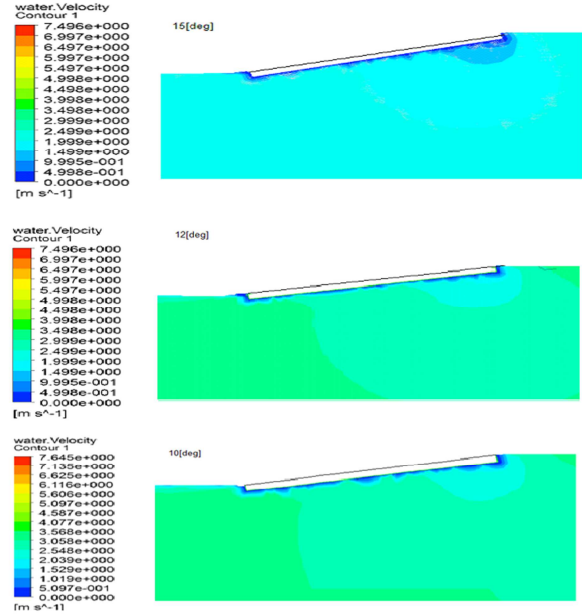
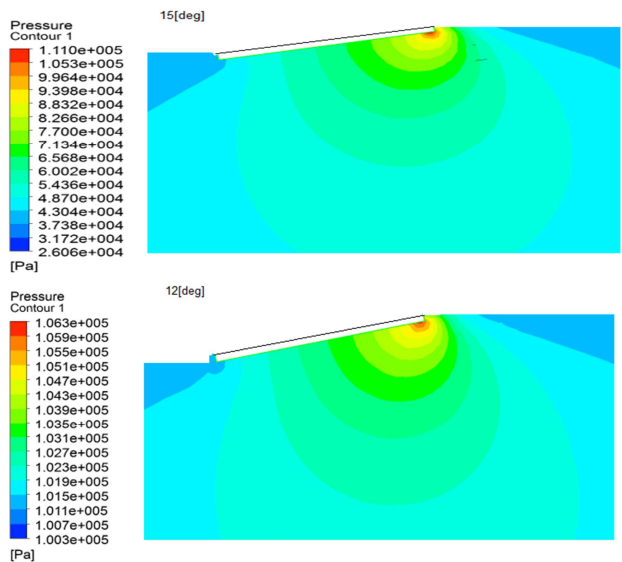


Figure.10: Velocity contours at fixed Fr= 1.1 for varying AOA



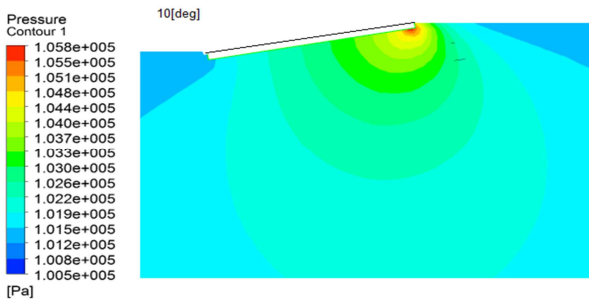


Figure.11: Plots of pressure contours for various AOA (Fr= 1.1)

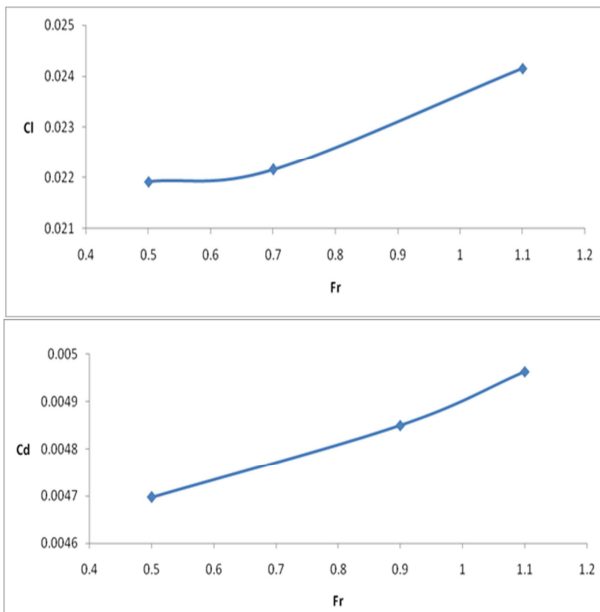


Figure.12: a) Lift coefficient as a function Fr at AOA=7.5°. b) Drag coefficient as a functions of Fr, AOA = 7.5°.

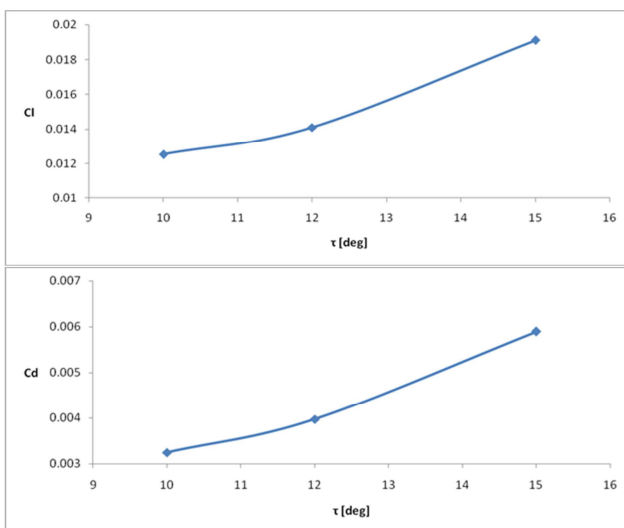


Figure.13: a) Lift coefficient as a function of AOA b) Drag coefficient as a functions of AOA (Fr= 1.1)

6.0 CONCLUSION

Numerical computations were conducted in this study for planing flat-plate, and pressure distributions, lift and drag, wave surface were predicted. Mesh dependency is shown that for the resent method 140000 meshes are enough. Pressure distribution is well matched with Kramer et-al results. Free surface profiles are determined at various Froude number and AOAs. High pressure is predicted at leading edge of the plate and low pressure at trailing edge. At high Froude number, it is clear observed that more free surface disturbances is shown at downstream of plate.

REFERENCES

- [1]. Doctors, L. J. 2009. *A study of the resistance characteristics of surface-effect-ship seals. Proc high-Performance Marine-Vehicle Symposium*, Linthicum, Maryland.
- [2]. Faltinsen, O. M. 2005. *Hydrodynamics of high-speed marine vehicles*, Cambridge University Press.
- [3]. Brown P.W. 1954. *An Empirical Analysis of the Planing Characteristics of Rectangular Flat-Plates and Wedges*. Aeronautical Research Council.
- [4]. Payne, P. R. 1982. *The differences between a wing and a planing plate in two-dimensional flow*. Ocean Engineering VOL 9, PP: 441-453.
- [5]. Payne, P. R. 1990. *Planing and impacting plate forces at large AOAs*. Ocean Engineering, 17, PP: 201-233.
- [6]. Ou, Y. & Dong, W., 2012. Study on influencing factors of drag reduction by air layer to a flat-plate with bottom step. *The Twenty-second International Offshore and Polar Engineering Conference, International Society of Offshore and Polar Engineers*.
- [7]. Kramer, M., Maki, K. & Young, Y. 2013. *Numerical prediction of the flow past a 2-D planing plate at low Froude number*. Ocean Engineering, 70, PP: 110-117.
- [8]. Durante, D., Broglia, R., Maki, K. J. & Di Mascio, A. 2014. *A study on the effect of the cushion pressure on a planing surface*. Ocean Engineering, 91, PP: 122-132.
- [9]. Fridman, G. & Tuck, E. 2006. *Two-dimensional finite-depth planing hydrofoil under gravity*. Proc. Third International Summer Scientific School, "High Speed Hydrodynamics and Numerical Simulation", Kemerovo, Russia.